

# Breast cancer histological images nuclei segmentation and optimized classification with deep learning

Fawad Salam Khan<sup>1,2</sup>, Muhammad Inam Abbasi<sup>3</sup>, Muhammad Khurram<sup>4</sup>, Mohd Norzali Haji Mohd<sup>1</sup>,  
M. Danial Khan<sup>2</sup>

<sup>1</sup>Faculty of Electrical and Electronic Engineering, Universiti Tun Hussain Onn Malaysia, Parit Raja, Malaysia

<sup>2</sup>Department of Machine Learning Automation, CONVSYS (Pvt) Ltd, Islamabad, Pakistan

<sup>3</sup>Faculty of Electrical and Electronic Engineering, Universiti Teknikal Melaka, Melaka, Malaysia

<sup>4</sup>University of Technology and Applied Sciences in Nizwa, Nizwa, Sultanate of Oman

## Article Info

### Article history:

Received Mar 29, 2021

Revised Mar 24, 2022

Accepted Apr 18, 2022

### Keywords:

Breast cancer

Histological images

Mask regional convolutional network

Nuclei

Segmentation

## ABSTRACT

Breast cancer incidences have grown worldwide during the previous few years. The histological images obtained from a biopsy of breast tissues are regarded as being the highest accurate approach to determine whether any cells exhibit symptoms of cancer. The visible position of nuclei inside the image is achieved through the use of instance segmentation, nevertheless, this work involves nucleus segmentation and features classification of the predicted nucleus for the achievement of best accuracy. The extracted features map using the feature pyramid network has been modified using segmenting objects by locations (SOLO) convolution with grasshopper optimization for multiclass classification. A breast cancer multi-classification technique based on a suggested deep learning algorithm was examined to achieve the accuracy of 99.2% using a huge database of ICIAR 2018, demonstrating the method's efficacy in offering an important weapon for breast cancer multi-classification in a medical setting. The segmentation accuracy achieved is 88.46%.

*This is an open access article under the [CC BY-SA](https://creativecommons.org/licenses/by-sa/4.0/) license.*



## Corresponding Author:

Muhammad Inam Abbasi

Department of Electrical and Computer Engineering, Universiti Teknikal Malaka  
Melaka, Malaysia

Email: inamabbasi@utem.edu.my

## 1. INTRODUCTION

The development of deep neural networks (DNN), researchers have become capable of identifying the illness with close accuracy rather of standard mammography approaches for breast cancer diagnosis [1]. Breast cancer is a leading cause of death among women. Cancer in its early detection reduces the mortality rate from breast cancer. The accuracy of diagnosis of cancer was raised, and the expense was decreased, thanks to the use of a computer-aided diagnostics systems. Conventional breast cancer classifying systems are built on handmade characteristics, and its success is dependent on the features picked. They are also extremely sensitive to differences in size and complicated forms. Histological breast cancer pictures, on the other hand, have a very complicated structure. Deep learning methods are now becoming an alternate method for diagnosis, overcoming the disadvantages of traditional classification approaches. While deep learning has done well in a variety of computer vision and pattern recognition applications, so it faces several difficulties. One of the most significant issues is a shortage of training data. To overcome this issue and boost efficiency, we used a transfer learning methodology, wherein deep learning models trained on one task and afterward fine-tune the model for the other [2].

Pathologic exams are the gold level in medical procedures as well as the law, and they necessitate specific action throughout the diagnosing procedure image classification may now benefit as from information analysis by hematoxylin and eosin-stained pictures, thanks to advancements in digital pathology. Despite this, it is reported with in bulk of breast cancer databases, making prediction studies more difficult. The goal of this project is to assess the efficacy of machine learning and deep learning approaches used to forecast breast cancer risk of recurrence. The research begins with a review of tissue preparations, stained imaging techniques, then cancer sufferer prognosis. In term of sensitivity and specificity, the high precision findings are reduced. The concerns of the absent loss function and class imbalances are generally ignored, and the effectiveness metrics used are context inappropriate. The issue is to analyze slide pictures for the needed contents imaging with diagnostic biomarkers and prognosis assistance provided by digital pathology [3].

A few of the convolutional neural network (CNN)-based categorization investigations have made extensive use of breast cancer histopathology database (break-his). This dataset was also utilized in the present research. The break-his dataset's histopathology pictures feature fine-grained looks and are hard to characterize. To increase accuracy of classification, it is crucial to highlight picture features and much more local knowledge. As a result, we suggest a structure based on interlaced Dense-Net and SENet (IDS-Net) to address the issue. Dense-Net can improve feature distribution and SENet can improve features extraction efficacy, the suggested IDS-Net not only uses detailed data with increased complexities and moreover integrates shallower information. Furthermore, in the classification network, the IDS-Net design employs global average pooling to offset the shortage of computational resource and network over-fitting induced by the enormous set of parameters [4]. The high preference of the computer-aided design (CAD) system offers automatic image analysis avoiding massive misdiagnosis which may cater the involvement radiologist's deficiency of practice for the diagnosis of histological images. In accumulation, money can be saved by expecting to avoid dual analysis by pathologist when considering single interpretation from the CAD system [5].

Image segmentation is a critical problem in computer vision and image processing, with multiple applications. In this context, the widespread success of deep learning (DL) has inspired the research on new image segmentation algorithms based on DL models covering convolutional pixel-labeling networks, encoder-decoder designs, multiscale and pyramid-based techniques, recurrent networks, visual attention models, and adversarial generative models. The relationships, strengths, and problems of different DL-based segmentation models has been analyzed, as well as frequently used datasets were reviewed, performances were compared, and intriguing research directions were identified. Image segmentation techniques deep learning-based models were examined that have shown excellent performance in a variety of image segmentation challenges and standards. For tackling optimization issues, grasshopper is suggested approach mathematically simulated as well as simulated the behavior of grasshopper swarming in nature. It is successfully located the potential areas of a particular search area. They experience sudden, huge alterations in the early stages of optimizations that aided them in searching worldwide. In the last stages of optimizations, grasshoppers likely to migrate locally, allowing them to use the searching area. Because of the fluctuating comfortable region coefficient, they must progressively balance exploitation and exploration, allowing grasshopper optimization algorithm (GOA) to avoid becoming locked in optimal solution and instead discover an approximate solution of the best solution. The GOA algorithm improved the average health of grasshoppers, demonstrating that it can successfully enhance the randomly initialized community of grasshoppers. The endurance of the goal improved with time, indicating that the estimate of the best solution grew more precise proportionate to the amount of iterations [6]. Figure 1 shows the four classes of breast cancer from the histological dataset ICIAR 2018 where Figure 1(a) is benign class, Figure 1(b) is the normal class, Figure 1(c) is the in-situ, and Figure 1(d) is the invasive class. The contributions of the research are: i) the features extracted from the feature pyramid network has been optimized by integrating state of art grasshopper optimization algorithm; ii) the optimized features are used after fully connected layers to improve the segmentation using segmenting objects by locations (SOLO) CNN model.

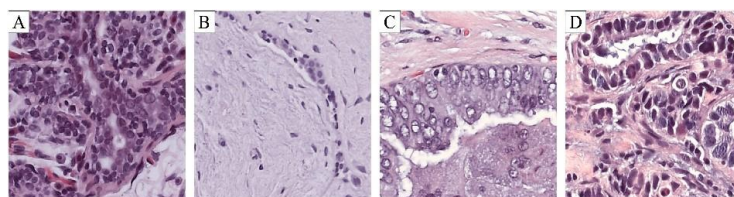


Figure 1. Breast cancer histological images (a) benign (b) normal (c) in-situ (d) invasive

Individuals having breast cancer are more likely to have significant health problems that lead to an increased death rate. The major cause could be radiologists; misunderstanding of worrisome lesions owing to technological difficulties with image quality and diverse breast density that raises the false (positive and negative) ratios. Numerous deep learning techniques for accurate breast cancer diagnosis and classifications were explored. Furthermore, computer-aided imaging analysis for improved picture interpretation is a time honored method in the healthcare computing area [7]. Many studies and surveys have been conducted in this regard. The advantages and dangers of breast multi-imaging modality, segmentation techniques, extraction of features, and classifications of breast disorders have been studied using cutting-edge deep learning techniques. Several famous sources were searched using the term breast cancer to offer a complete assessment on current diagnostics methods and to broaden research issues for radiologist and scholars. As demonstrating the methods efficacy in offering an important weapon for breast cancer multi-classification in medical setting. This issue too is classified by taxonomy [8]. Despite the fact that the prevalence of breast cancer has increased dramatically in recent years, the mortality rate has fallen significantly [9]. This decrease in fatalities has primarily happened in industrialized nations. Those making significant advances in early diagnosis approaches using clinical imagery analysis in particular [10]. In general, histological biopsy testing is by far the most reliable method of diagnosing breast cancer. Pathologists use tiny needle ejected slides of breast tissue to perform the technique. A variety of breast tissue slides are examined at different microscopy magnification settings for every individual in order to correctly assess regions of interest (ROIs). Nonetheless, pathologist' interpretations are frequently influenced by human variables like eye tiredness, as well as device-specific effects. To minimize the chances of endangering a life of a patient, domain specialists outsource this duty to computer aided diagnosis (CAD) techniques [11]–[14], that are being improved by a vast research field. Nonetheless, manually multi-classification for histological pictures of breast cancer remains a significant issue. So, there are 3 primary causes for this: (i) Pathologist' specialized backgrounds and extensive expertise have become so challenging to acquire or invent those basic clinics and hospitals lack a lot of qualified pathologists; (ii) the laborious work is costly and complex; and (iii) pathologists' tiredness may lead to misdiagnosed. As a result, it is critical to employ computer-aided breast cancer multi-classification, that can decrease pathologist' high responsibilities and assist minimize misdiagnosis [15]–[17].

These technologies are used to improve picture qualities for personal assessment as well as to automating picture reading for improved comprehension and understanding. Several studies on breast cancer detection, segmentation, and classification utilizing machine learning and artificial intelligence (AI) approaches have recently been reported [18], [19]. Most prior work focused on machine learning (ML) systems that used binary classification to diagnose cancers. A unique deep learning-based approach for breast cancer detection and classification utilizing mammographic imaging has been suggested [20]–[22] a deep learning-based methodology for classifying breast tumors lacking lesions segments and selection of the features. In [23] reduced the computing complexity of all forms of mammographic pictures to conduct breast cancer binary classification. Used binary classification to derive morphological characteristics from ultrasonography pictures. Youk *et al.* [24] introduced a novel ultrasonography method called elastography to distinguish between benign and malignant breast tumor lesion. The [25] used magnetic resonance imaging (MRI) modality to develop deep-learning-based methods for questionable region-of-interest (ROI) segmentation and categorization.

## 2. PROPOSED METHOD

The images are fed into the conventional convolution networks. ResNet50 and ResNet101 that serve as backbone network for extracting features for precision computation. This network is mostly utilized for extracting features, detecting fundamental characteristics such as edges. Combining feature pyramid networks yields high level features (FPN) used for high level features extractions. The input histological image is divided into a grid of  $S \times S$  cells. If the center of an object falls in a grid cell, then the grid cell predicts the semantic category and assigns location information for each pixel. It has two branches i.e. the category branch and mask branch [26].

### 2.1. Mask kernel branch

The mask kernel branch is located in the prediction head, together with the semantic category branch. The prediction head works on the feature map pyramid output by FPN. The two branches in the head consist of 4 convolutions for feature extraction, and the last convolution is used for prediction. The weight of the Head is shared on different feature layer levels. The author adds the spatial function to the kernel branch by adding normalized coordinates to the first convolution, that is, connecting two additional input channels. For each grid, the D-dimensional output of kernel branch prediction represents the predicted convolution kernel weight, where D is the number of parameters. When in order to generate the weight of  $1 \times 1$  convolution with E input channels,  $D=E$ , and when  $3 \times 3$  convolution  $D=9E$ . These generated weights depend

on the location, the grid unit. If the input image is divided into  $S \times S$  grids, the output space will be  $S \times S \times D$ . Note that no activation function is needed here. Here the input is the feature  $F$  of  $H \times W \times E$ , where  $E$  is the number of channels of the input feature; the output is the convolution kernel  $S \times S \times D$ , where  $S$  is the number of grids divided, and  $D$  is the number of channels of the convolution kernel. The corresponding relationship is:  $1 \times 1 \times E$  convolution kernel, then  $D=E$ ,  $3 \times 3 \times E$  convolution kernel, then  $D=9E$ .

## 2.2. Mask feature branch

The process of decoupled mask kernel with the isolated separated prediction, there are two ways to construct mask feature branch:

- Mask features are predicted for each FPN level: you can put it in the head together with the Kernel branch, which means we can predict the mask features of each FPN level
- The mask feature representation of the unified prediction technique for all FPN levels: predict a unified mask feature representation for all FPN levels

## 2.3. Features extraction and optimization

Feature extraction is a method of reducing dimensions that efficiently depicts reduced feature vectors. When dealing with enormous image sizes, this method comes in handy. The quantitative evaluation of tissues and organs functioning is dependent on obtaining appropriate information to define cell and tissues architecture. Morphology, textural, co-localization, as well as regionally associated variables are calculated to assess deviation across cells and tissues structure. Form, dimension, and colors are examples among both locally and globally characteristics. Local features are utilized for object detection identification as well as the identification of blob, edges, and edges pixel, whereas global features are utilized for images retrieving, object recognition, and classification. Some of the methods are morphometrically features, color intensity based factors, textural features, the real daubechies wavelet transform, the dual tree complex wavelet transform, fractal texture features, and the handcrafted features. The searching is conceptually divided into two inclinations by nature inspired methodologies, which is exploration and exploitation. The searching units are urged to travel suddenly while exploration, whereas they typically shift locally while exploitation. As a result, if we could somehow mathematically represent this behavior, we can create a new nature-inspired algorithm. The mathematical formula used to mimic grasshopper swarming type of behavior is shown:

$$Z_j = D_j + F_j + B_j \quad (1)$$

where, the  $Z_j$  describes the place of the  $j$ -th grasshopper,  $D_j$  for the social interaction,  $F_j$  for the gravity force on the  $j$ -th grasshopper, and  $B_j$  illustrates the wind advection. The equation is defined to offer the random behavior:

$$D_j = \sum_{\substack{i=1 \\ i \neq j}}^N g(h_{ji}) h_{ji}^{\wedge} \quad (2)$$

where,  $h_{ji}$  defines the distance among the  $j^{\text{th}}$  and  $i^{\text{th}}$  grasshopper,  $g$  defines the power of social forces, and  $h_{ji}^{\wedge}$  behaves as a unit vector between the  $j$ -th grasshopper to the  $i$ -th grasshopper.

The variable  $g$  is presented to demonstrate how it affects grasshopper socializing (appeal and repel). Social forces are calculated as:

$$g(s) = f e^{\frac{-s}{p}} - e^{-s} \quad (3)$$

The components of (1) can be solved:

$$F_j = -l e_i^{\wedge} \quad (4)$$

$$B_j = v e_n^{\wedge} \quad (5)$$

As a result, this equation has been used to mimic the interactions of grasshoppers in a swarm. This equation is shown to drive the original randomized group close together till they create a unified, controlled swarm. Putting the values of  $F_j$ ,  $B_j$ , and  $D_j$  in (1), we get:

$$Z_j = \sum_{\substack{i=1 \\ i \neq j}}^N g(|x_i - x_j|) \frac{x_i - x_j}{h_{ji}} - l e_i^{\wedge} + v e_n^{\wedge} \quad (6)$$

The numerical equation, therefore, can be utilized straight to resolve optimization issues, owing to the fact that the grasshoppers soon find their safe zone and also the swarm doesn't really converge to a specific spot so, to tackle optimization difficulties, the following revised version of the equation is formulated:

$$Z_j^d = c \left( \sum_{\substack{i=1 \\ i \neq j}}^N c \frac{ub_d - ub_{qd}}{2} g(|x_i^d - x_j^d|) \frac{x_i - x_j}{h_{ji}} \right) + T_d^{\wedge} \quad (7)$$

To balance exploitation and exploration, the variable  $c$  must be reduced according to the number of iterations. As the number of iterations rises, this process encourages exploitation. The coefficient  $c$ , which is proportional to the number of iterations, is computed as shown:

$$c = cmax - k \frac{cmax - cmin}{K} \quad (8)$$

where  $cmax$  denotes the greatest value,  $cmin$  denotes the minimum value,  $k$  is the current iteration, and  $K$  denotes the highest no. of iterations. These implementations have the relevant conclusions where the features are refined during the iteration process, thus the estimate of the global optimum became more precise according to the iteration. GOA has address features optimization problem using unidentified search terms. The findings revealed that the suggested method outperformed well known and current techniques in this research. Lastly, the right choice provided by the swarm thus far was chosen as a goal to really be pursued and refined by the grasshoppers. Figure 2 shows the block diagram of the complete methodology.

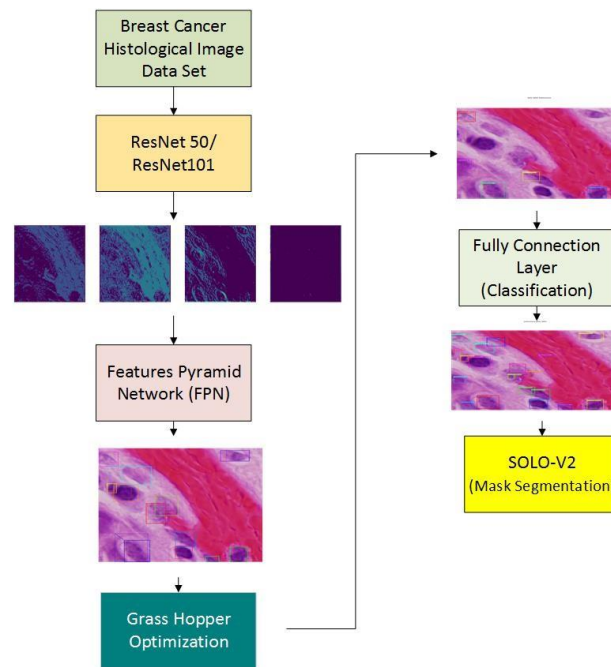


Figure 2. Block diagram

#### 2.4. Dataset

The collection contains 400 images of breast histology images divided into four categories: normal, benign, in-situ, and invasive. Every picture has a resolution of 512 by 512 pixels. Every class has 100 photos, as well as the nuclei's boundary boxes are supplied with in shape of polygons. The augmentation approach (mirroring and rotation) was used, yielding 1908 pictures.

#### 2.5. Data preparation

The data was separated among train and validity batches with every class receiving 80% of the photos for training and the remaining percent for validation. This equates to 80 and 20 photos for the two datasets, respectively. Throughout testing and training, the initial size of 512×512 pixels was kept.

## 2.6. Pre-processing

To minimize overfitting, picture augmentation was used, in which every picture was enhanced by mirrored and rotating it to 45°, 60°, 135°, and 270°. This stage yielded 477 photographs to every class, for a sum of 1,908 photos. To prevent the chance of overlapping, the augment phase was conducted following splitting the train and test sets.

## 2.7. Segmentation and nuclei localization

An image segmentation model should ideally be assessed in a variety of ways, including quantitative accuracy, visual quality, speed, and storage needs. To yet, however, most academics have concentrated on measures for assessing model accuracy. The following are the most commonly used metrics:

- a. Pixel accuracy is defined as the ratio of classified pixels divided by the total no. of pixels,

$$PA = \frac{\sum_{j=0}^L p_{jj}}{\sum_{j=0}^L \sum_{i=0}^L p_{ji}} \quad (9)$$

where,  $p_{ji}$  is the no. of pixels of class  $j$  foreseen as belonging to class  $i$ .

- b. Mean pixel accuracy (MPA) is defined as an extension of the PA in which the ratio of correct pixels is calculated per class and then averaged over total no. of classes:

$$MPA = \frac{1}{L+1} \sum_{j=0}^L \frac{p_{jj}}{\sum_{i=0}^L p_{ji}} \quad (10)$$

- c. Intersection over union (IoU) is defined as the area of intersection in between predicted segmentation map A and the ground truth map B, divided by the area of union in between two maps, and ranges between 0 and 1:

$$IoU = I(C, D) = \frac{|C \cap D|}{|C \cup D|} \quad (11)$$

- d. Precision/Recall/F1 scores can be defined separately for each class and also for the aggregate level, as shown:

$$Precision = \frac{AB}{AB+CB} ; \quad Recall = \frac{AB}{AB+CD} \quad (12)$$

where, AB denotes to true positive fraction, CB denotes to false positive fraction, and CD denotes to false negative fraction.

- e. Q1 score can be defined as the harmonic mean of precision and recall:

$$Q1 = \frac{2 \text{ Precision Recall}}{\text{Precision} + \text{Recall}} \quad (13)$$

- f. Dice coefficient, which is often employed in medical image analysis, is defined as the overlap area of the predicted and ground-truth maps divided by the total number of pixels

$$Dice = \frac{2 |C \cap D|}{|C| + |D|} \quad (14)$$

## 2.8. Classification

Classifiers are accessible for multiclass classification; soft-max regression approach was utilized to categorize benign, in-situ, invasive, and normal throughout the datasets. To get the high-performance task for classification to achieve good feature representation for the labeled data of hematoxylin-eosin-stained breast biopsy images used with the help of support vector machine. The model consists of fully connected layers and convolutional layers and pooling layers reduces the output dimensions for classification.

## 3. RESULTS

We have calculated an  $N \times N$  pairwise IoU matrix for every presiding value to  $N$  values in descending order to achieve the score. For the binary mask, the IoU matrix used to realize through matrix operations. The IoU with the maximum number of overlapping columns on the  $N \times N$  matrix calculated. Then calculate all the attenuation factors predicted by the higher scores and select each predicted attenuation factor

as the most effective attenuation factor through the minimum value of each column. Finally, the score is updated by the attenuation factor. We computed the shifting as well as resizing to have the anchor entirely enclose the grounds truth entity when training the FPN repressors. For refining of the histology imaging, we employed the Keras modeling to activate the FPN graphs in which the attributes from the GOA were merged, and afterwards we utilized non max suppressing to prevent excessive recognition of same entity. The implementation of the classifiers head upon suggestions that build bounding box regression model and class probability. Next, through utilizing filter low confidence detecting, bounding box refining was used to remove the backgrounds for the identified nucleus. The mask head creates segmented masking per each instance of the histology images using the detection systems (polished bounding box coordinates and classification IDs for benign, in situ, invasion, and regular breast cancer categories) from the preceding phase. The backbone networks were analyzed to use the ResNet50 as well as ResNet101 SOLO CNN architectures. That is clear that because the number of iterations rises, the losses decrease in an inversely logarithmic way. The outcomes of all levels, therefore, significantly superior in regards of losses than that of the outcomes of heads. The regional convolutional network levels as well as the head of the mask are basically separated between two sections. In 70 iterations, the outcome was seen. The person in charge of the system’s segments and categorization of histology images.

**3.1. Experimental setup**

The experimental scheme involves a Core i7 PC with 24 GB RAM and also an Nvidia 1080Ti GTX GPU. The deployment tool was Anaconda with Jupyter Notebook, using Tensor-Flow and Keras it as machine learning platform and library. We utilized SOLO V2, which was built with open-source materials. It is distributed underneath the license of Massachusetts Institute of Technology (MIT). Both Resnet50 and Resnet101 were employed as that of the network’s backbone in installation. ResNet101 and ResNet 50 are the two different backbone networks where loss calculated on 40 number of iterations, the graph is composed of all layers and the head values as shown in Figures 3 and 4. The more convolution layers in ResNet 101 shows the better converges and minimize smoothly as compared to ResNet50.

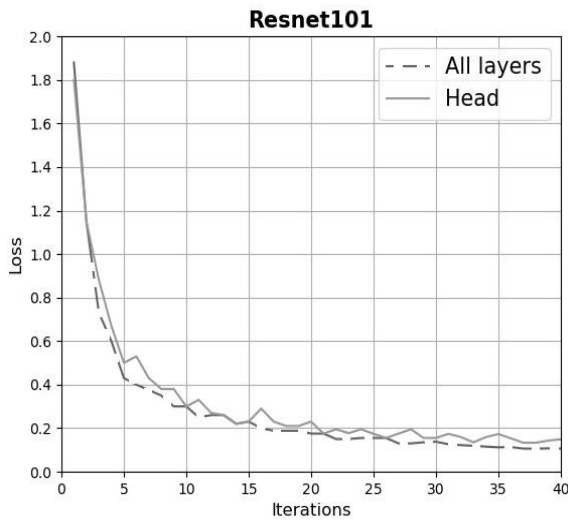


Figure 3. ResNet101

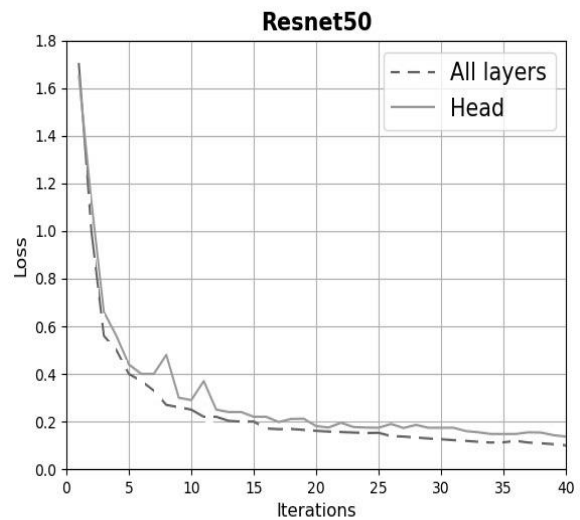


Figure 4. ResNet50

**3.2. Segmentation of histological images**

Each bounding box when annotated have different number of pixels where overlap coefficient demonstrates the ratio of pixels marked for that defined bounding box. The two different backbones ResNet101 and ResNet50 are utilized in the research to calculates the overlap coefficient with the different average precision scales. Average precision can be calculated using these overlap coefficient (OC) as shown in the Table 1.

Table 1. Overlap coefficient

Backbone	AP 0.5	AP 0.75	AP 0.9	Overlap Coefficient
ResNet 50	1	0.9667	0.2334	0.8776
ResNet 101	1	0.9166	0.355	0.8846

The Figure 5 demonstrates the result of mask generated on the annotated area of the different regions of the histological images. The various marked segmented areas are then used to classify the type of breast cancer. In SOLO segmentation technique, biopsy images used to show dominance and classify the image segmentation method in this result.

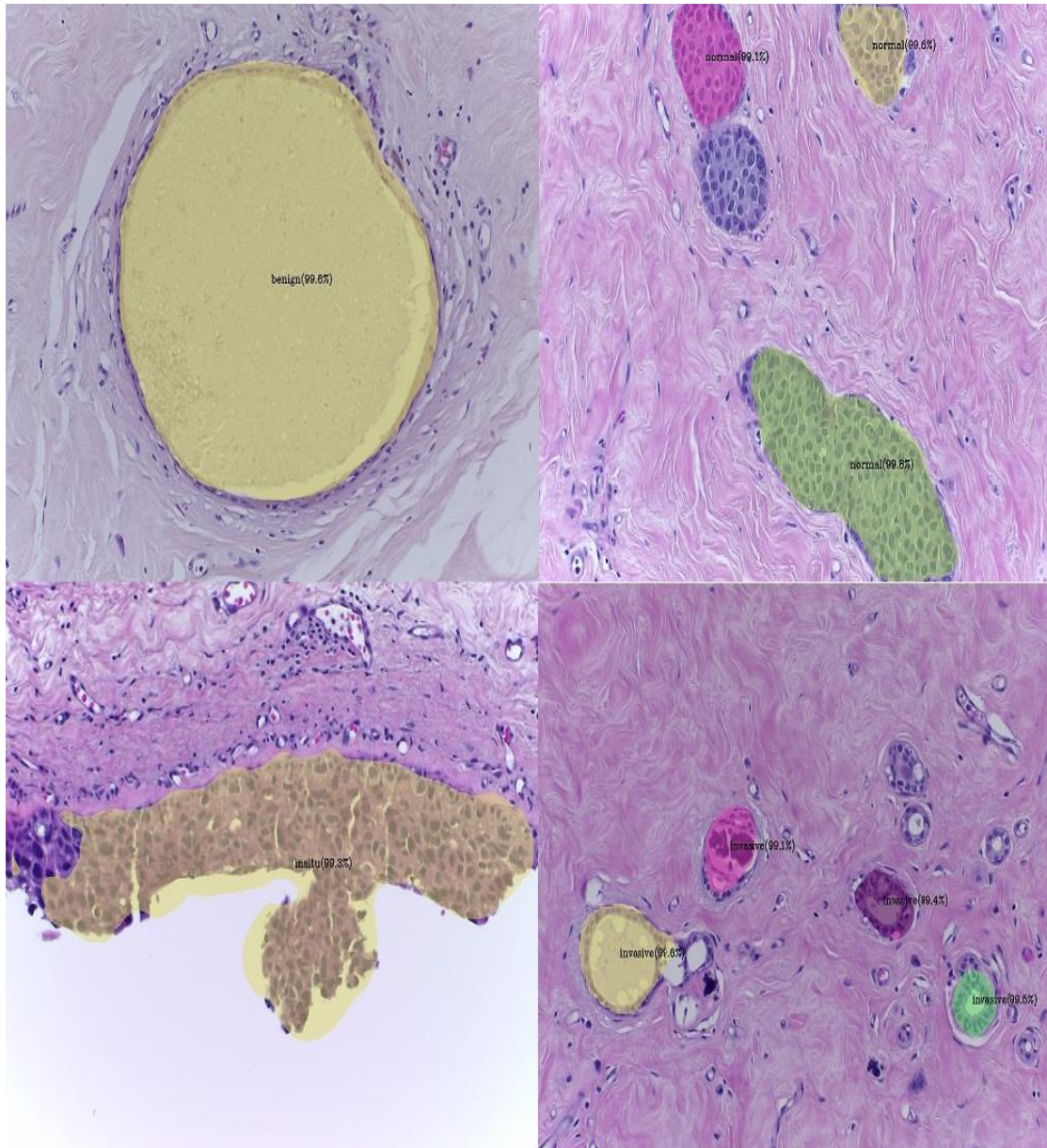


Figure 5. Mask generation during segmentation (a) benign (b) normal (c) invasive and (d) in-situ cancer

### 3.3. Validation loss and confusion matrix

Training on network using ICIAR dataset for breast cancer histological images where the fraction of pixel belonging to targeting truth bounding box is appropriately split into the background after networks training that use the ICIAR dataset for breast cancer histology imaging. Because of the very stochastic character of cancer diagnosis, the outcome in loss was already noticed in validation loss for the same number of iterations, which is how the behavior is loss variable. Because to the little amount of fluctuation and changes, the graph was drawn on a half logarithmic scale across the Y-axis. In the training dataset, the loss was reduced to 0 within 30 rounds. The effect of breast cancer categorization as indicated in the confusion matrices. The test datasets had 95 images out of each category.

The validation accuracy calculated on 30 iterations and it found quite obvious that due to stochastic nature of the histological images, the spikes are normalized and converge near to 1 as shown in Figure 6. The x-axis describes the number if iterations and the y-axis show the loss values. There are 95 images of each class used for the testing where the mis-classes observed is 0.0079 as shown in the confusion matrix in Figure 7.

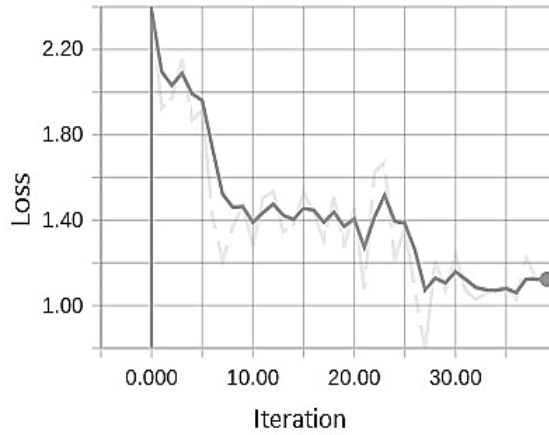


Figure 6. Validation loss

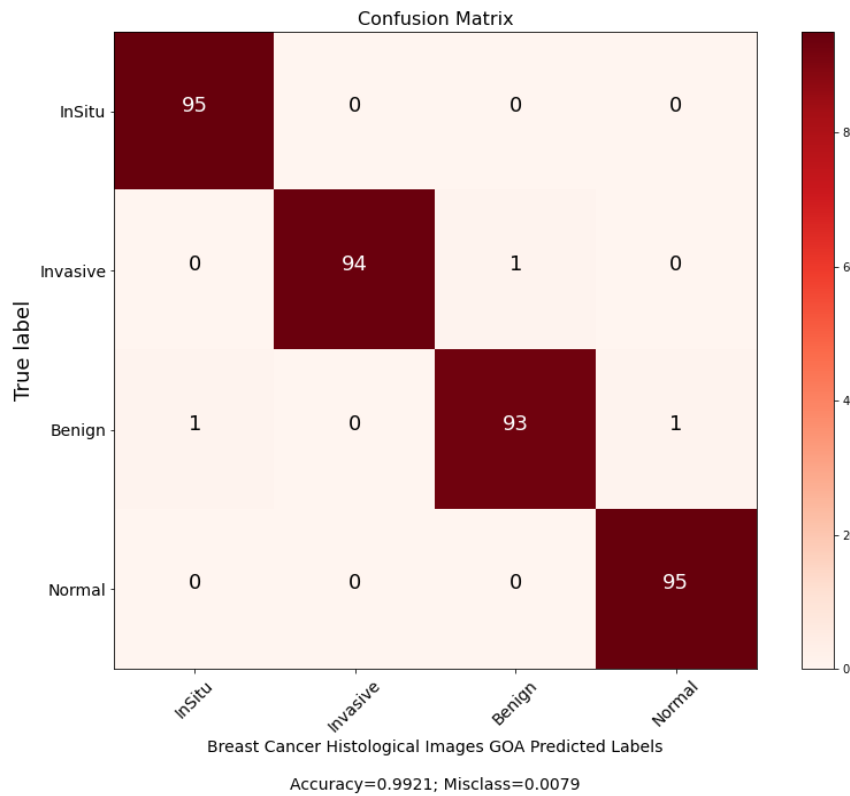


Figure 7. Confusion matrix with optimization

### 3.4. Comparative analysis

The proposed method evaluated for the comparison with the available research for the accuracy and segmentation on the similar datasets. Mask regional convolution network (MASK-RCNN) and convolutional

neural networks (CNN) using the dataset of ICIAR 2018. Although results show better accuracy and segmentation for the proposed method using the optimization technique as shown in Table 2.

Table 2. Comparative analysis for accuracy and segmentation

Paper	Method	Dataset	Accuracy	Segmentation
Khan <i>et al.</i> [1]	Mask-RCNN	ICIAR 2018	98.16 %	86.39%
Alzubaidi <i>et al.</i> [2]	CNN	ICIAR 2018	96.10 %	NA
Proposed Method	SOLO+GrassHopper	ICIAR 2018	99.20 %	88.46

#### 4. DISCUSSION

When comparing to various models lacking segmentation, the segmentation strategy utilizing SOLO V2 showed the dominance as compared to other segmentation models. The mask RCNN model [1] has an accuracy of classification of 98.16% in breast cancer histology images that is higher to models whereas the accuracy achieved using SOLOV2 with optimized features from grass hopper optimization is 99.21%. Within 30 iterations on GPU training, the validation loss approach towards zero. The backbone network ResNet50 outperforms ResNet101 at extracting features in 40 epochs (iterations) and has lower computing costs owing to fewer convolution layers. Preprocessing enhancements lowered the likelihood of overfitting by increasing the picture datasets from 400 to 1,908 (477 to every class). The findings exceeded the most recent approaches created for the ICIAR 2018 dataset's breast cancer classification task. We want to employ the same domain to further implement using other newly designed CNN model which can further conceptualized the enhancement of the efficiency of other challenges as the future work because it may further increase the efficiency of the breast cancer classification job.

#### 5. CONCLUSION

It has been quite evident that breast cancer diagnosis using the histological images is very hectic task for pathologists. Deep learning methods has proved dominance and provide best accuracy for the classification of different types of breast cancer. The method proposed using publically available dataset ICIAR 2018 gives the best accuracy and segmentation method for the provision of less errors during the diagnosis process.

#### ACKNOWLEDGEMENTS

The authors would like to thank the Centre for Research and Innovation Management (CRIM), Universiti Teknikal Malaysia Melaka (UTeM) for the financial support of this work.

#### REFERENCES

- [1] F. S. Khan, M. N. H. Mohd, M. D. Khan, and S. Bagchi, "Breast cancer histological images nuclei segmentation using mask regional convolutional neural network," in *2020 IEEE Student Conference on Research and Development (SCoReD)*, Sep. 2020, vol. 2020-Janua, pp. 1–6, doi: 10.1109/SCoReD50371.2020.9383186.
- [2] L. Alzubaidi, O. Al-Shamma, M. A. Fadhel, L. Farhan, J. Zhang, and Y. Duan, "Optimizing the performance of breast cancer classification by employing the same domain transfer learning from hybrid deep convolutional neural network model," *Electronics*, vol. 9, no. 3, p. 445, Mar. 2020, doi: 10.3390/electronics9030445.
- [3] R. Krithiga and P. Geetha, "Breast cancer detection, segmentation and classification on histopathology images analysis: a systematic review," *Archives of Computational Methods in Engineering*, vol. 28, no. 4, pp. 2607–2619, Jun. 2021, doi: 10.1007/s11831-020-09470-w.
- [4] X. Li, X. Shen, Y. Zhou, X. Wang, and T.-Q. Li, "Classification of breast cancer histopathological images using interleaved DenseNet with SENet (IDSNet)," *PLOS ONE*, vol. 15, no. 5, p. e0232127, May 2020, doi: 10.1371/journal.pone.0232127.
- [5] S. Bagchi, K. G. Tay, A. Huong, and S. K. Debnath, "Image processing and machine learning techniques used in computer-aided detection system for mammogram screening-a review," *International Journal of Electrical and Computer Engineering (IJECE)*, vol. 10, no. 3, pp. 2336–2348, Jun. 2020, doi: 10.11591/ijece.v10i3.pp2336-2348.
- [6] S. Saremi, S. Mirjalili, and A. Lewis, "Grasshopper optimisation algorithm: theory and application," *Advances in Engineering Software*, vol. 105, pp. 30–47, Mar. 2017, doi: 10.1016/j.advengsoft.2017.01.004.
- [7] T. Mahmood, J. Li, Y. Pei, F. Akhtar, A. Imran, and K. U. Rehman, "A brief survey on breast cancer diagnostic with deep learning schemes using multi-image modalities," *IEEE Access*, vol. 8, pp. 165779–165809, 2020, doi: 10.1109/ACCESS.2020.3021343.
- [8] Y. Li, J. Wu, and Q. Wu, "Classification of breast cancer histology images using multi-size and discriminative patches based on deep learning," *IEEE Access*, vol. 7, pp. 21400–21408, 2019, doi: 10.1109/ACCESS.2019.2898044.
- [9] J. Ferlay *et al.*, "Cancer incidence and mortality worldwide: Sources, methods and major patterns in GLOBOCAN 2012," *International Journal of Cancer*, vol. 136, no. 5, pp. E359–E386, Mar. 2015, doi: 10.1002/ijc.29210.
- [10] W. Liu, M. Juhas, and Y. Zhang, "Fine-grained breast cancer classification with bilinear convolutional neural networks

- (BCNNs),” *Frontiers in Genetics*, vol. 11, no. September, pp. 1–12, Sep. 2020, doi: 10.3389/fgene.2020.547327.
- [11] M. A. Aswathy and M. Jagannath, “Detection of breast cancer on digital histopathology images: Present status and future possibilities,” *Informatics in Medicine Unlocked*, vol. 8, no. November 2016, pp. 74–79, 2017, doi: 10.1016/j.imu.2016.11.001.
- [12] F. Ghaznavi, A. Evans, A. Madabhushi, and M. Feldman, “Digital imaging in pathology: whole-slide imaging and beyond,” *Annual Review of Pathology: Mechanisms of Disease*, vol. 8, no. 1, pp. 331–359, Jan. 2013, doi: 10.1146/annurev-pathol-011811-120902.
- [13] M. N. Gurcan, L. E. Boucheron, A. Can, A. Madabhushi, N. M. Rajpoot, and B. Yener, “Histopathological image analysis: a review,” *IEEE Reviews in Biomedical Engineering*, vol. 2, pp. 147–171, 2009, doi: 10.1109/RBME.2009.2034865.
- [14] Z. Hu, J. Tang, Z. Wang, K. Zhang, L. Zhang, and Q. Sun, “Deep learning for image-based cancer detection and diagnosis-A survey,” *Pattern Recognition*, vol. 83, pp. 134–149, Nov. 2018, doi: 10.1016/j.patcog.2018.05.014.
- [15] Y. Zheng, J. Yu, C. Kambhamettu, S. Englander, M. D. Schnall, and D. Shen, “De-enhancing the dynamic contrast-enhanced breast MRI for robust registration,” in *Medical Image Computing and Computer-Assisted Intervention-MICCAI 2007*, vol. 4791 LNCS, no. PART 1, Berlin, Heidelberg: Springer Berlin Heidelberg, 2007, pp. 933–941.
- [16] Y. Cai, M. Landis, D. T. Laidley, A. Kornecki, A. Lum, and S. Li, “Multi-modal vertebrae recognition using transformed deep convolution network,” *Computerized Medical Imaging and Graphics*, vol. 51, pp. 11–19, Jul. 2016, doi: 10.1016/j.compmedimag.2016.02.002.
- [17] Y. Zheng, B. Wei, H. Liu, R. Xiao, and J. C. Gee, “Measuring sparse temporal-variation for accurate registration of dynamic contrast-enhanced breast MR images,” *Computerized Medical Imaging and Graphics*, vol. 46, pp. 73–80, Dec. 2015, doi: 10.1016/j.compmedimag.2015.05.004.
- [18] G. Litjens *et al.*, “A survey on deep learning in medical image analysis,” *Medical Image Analysis*, vol. 42, no. 1995, pp. 60–88, Dec. 2017, doi: 10.1016/j.media.2017.07.005.
- [19] S. Duraisamy and S. Emperumal, “Computer-aided mammogram diagnosis system using deep learning convolutional fully complex-valued relaxation neural network classifier,” *IET Computer Vision*, vol. 11, no. 8, pp. 656–662, Dec. 2017, doi: 10.1049/iet-cvi.2016.0425.
- [20] M. Arfan, “Deep learning based computer aided diagnosis system for breast mammograms,” *International Journal of Advanced Computer Science and Applications*, vol. 8, no. 7, pp. 286–290, 2017, doi: 10.14569/IJACSA.2017.080738.
- [21] M. H.-M. Khan, “Automated breast cancer diagnosis using artificial neural network (ANN),” in *2017 3rd Iranian Conference on Intelligent Systems and Signal Processing (ICSPIS)*, Dec. 2017, vol. 2017-Decem, pp. 54–58, doi: 10.1109/ICSPIS.2017.8311589.
- [22] Y. Qiu *et al.*, “A new approach to develop computer-aided diagnosis scheme of breast mass classification using deep learning technology,” *Journal of X-Ray Science and Technology*, vol. 25, no. 5, pp. 751–763, Oct. 2017, doi: 10.3233/XST-16226.
- [23] vahid salimian Rizi, “Ce Pte Us Pt,” *Materials Research Express*, pp. 0–12, 2019.
- [24] J. H. Youk, H. M. Gweon, and E. J. Son, “Shear-wave elastography in breast ultrasonography: the state of the art,” *Ultrasonography*, vol. 36, no. 4, pp. 300–309, Oct. 2017, doi: 10.14366/usg.17024.
- [25] G. Amit, R. Ben-Ari, O. Hadad, E. Monovich, N. Granot, and S. Hashoul, “Classification of breast MRI lesions using small-size training sets: comparison of deep learning approaches,” in *Medical Imaging 2017: Computer-Aided Diagnosis*, Mar. 2017, vol. 10134, p. 10134IH, doi: 10.1117/12.2249981.
- [26] X. Wang, R. Zhang, T. Kong, L. Li, and C. Shen, “SOLOv2: Dynamic and fast instance segmentation,” in *Advances in Neural Information Processing Systems*, 2020, vol. 2020-Decem, no. NeurIPS, pp. 1–17.

## BIOGRAPHIES OF AUTHORS



**Fawad Salam Khan**    is currently doing PhD in Electrical Engineering from Universiti Tun Hussain Onn Malaysia. He received various gold and silver medals for different AI projects in Malaysia. He is an IEEE graduate student member and professional member of PEC Pakistan, completed BS Computer Engineering from SSUET Pakistan in 2002, ME Computer Engineering from NEDUET Pakistan in 2011 and MS Computer Science from IIUI Pakistan in 2020. He has more than 17 years of experience in industry and academia. Currently affiliated with Pakistan top AI Company CONVSYS (Pvt) Ltd. as the Director and CEO heading different AI, Machine and Deep Learning Projects of Silicon Valley (USA), Malaysia and UK. He is also teaching various computer engineering and computer sciences subjects in different universities in Pakistan. He can be contacted at email: he190038@siswa.uthm.edu.my.



**Dr. Muhammad Inam Abbasi**    completed his BSC in Electrical Engineering with major in Telecommunication in 2008 from Centre for Advanced Studies in Engineering (CASE Islamabad), University of Engineering and Technology (UET, Taxila), Pakistan. He joined Wireless and Radio Science Centre (WARAS), Universiti Tun Hussein Onn Malaysia (UTHM) as a Graduate Research Assistant in 2009 where he completed his Master by Research and Ph.D. in Electrical Engineering in 2011 and 2016 respectively. He worked as a post-Doctoral research fellow at Wireless Communication Centre (WCC), Universiti Teknologi Malaysia (UTM) from 2017-2018. Currently, He is working as a senior lecturer at the Faculty of Electrical and Electronic Engineering Technology, Universiti Teknikal Malaysia Melaka (UTeM). He can be contacted at email: inamabbasi@utem.edu.my.



**Dr. Muhammad Khurram**     is currently working as a Lecturer in University of Technology & Applied Sciences in Nizwa, Sultanate of Oman. He has 21 years of experience in academia, teaching and research. He received his Ph. D in Informatics from Malaysia University of Science and Technology, Malaysia. He completed his B.S and M.S in Computer Engineering both from Sir Syed University of Engineering and Technology in 1999 and 2002 respectively. He also teaches various Universities in Pakistan as an adjunct faculty member. He is also the life member of Pakistan Engineering Council, also he was the member National Curriculum Review Committee (NCRC) HEC Pakistan (2009-2012), he was the member technical committee, Information Technology Department Government of Sindh (2012-2015), also he was the member Board of Studies Computer Systems Engineering Department in Dawood University of Engineering and Technology, Karachi. He can be contacted at email: muhammad.khurram@nct.edu.om.



**Dr. Mohd Norzali Haji Mohd**     is currently working as Senior lecturer, Faculty Lab Manager (HoD) and Former Industrial Training Coordinator at the Department of Computer Engineering, Faculty of Electrical and Electronic Engineering, Universiti Tun Hussein Onn Malaysia (UTHM). He received Diploma in Computer Engineering from Toyama Maritime College, Japan in 2000 and B.Eng., M.Eng. from Fukui University, Japan in 2002 and 2004 respectively. In April 2015, he received Ph.D. from the Department of Information Sciences and Biomedical Engineering, Kagoshima University, Japan. He holds several research grants such as e-Science Fund in 2009, FRGS in 2008 and 2013, UTHM short term Grant in 2009 and 2010 MEXT-JSPS KAKENHI 2014 and GIPS in 2015. He participated in several research and innovation showcases “Automatic Moving Vehicle Recognition System” RMC 2008, 2nd Place, CCTET 2006 and IAPR MVA 2015. He has supervised 29 B.Eng., 2 M.Eng. and 55 Industrial training student. Currently supervising 4 B.Eng., 2 M.Sc., 2 PhD student. He can be contacted at email: norzali@uthm.edu.my.



**M. Danial Khan**     did BS Electrical Engineering from HITEC University Taxila, Pakistan. He is currently working in CONVSYS (Pvt) Ltd. Islamabad, Pakistan as the Design Engineer. He has 4 years of experience in designing AI Solutions for Silicon Valley, UK, and Malaysia. His major expertise in python, C++, TensorFlow, Keras and CNN Modeling. He has completed various projects like Automated AI Fitness Trainer, Fatigue Detection System, Fashion Design AI Pipeline using deep learning, Vehicle and number plates recognition system, and Automated AI Toolbox. He is also involved in training of AI, ML, and deep learning to customers in Pakistan as well as abroad. He can be contacted at email: danial.khan@convsys.net.